



Original contribution

The repertoire of genetic alterations in salivary duct carcinoma including a novel *HNRNPH3-ALK* rearrangement[☆]



Snjezana Dogan MD^{a,*}, Charlotte K.Y. Ng PhD^{a,b}, Bin Xu MD, PhD^a, Rahul Kumar PhD^a, Lu Wang MD PhD^a, Marcia Edelweiss MD^a, Sasinya N. Scott MPH^a, Ahmet Zehir PhD^a, Alexander Drilon MD^c, Luc G.T. Morris MD^{d,e}, Nancy Y. Lee MD^f, Cristina R. Antonescu MD^a, Alan L. Ho MD, PhD^c, Nora Katabi MD^a, Michael F. Berger PhD^{a,e}, Jorge S. Reis-Filho MD, PhD^{a,e}

^aDepartment of Pathology, Memorial Sloan Kettering Cancer Center, New York, NY 10065, USA

^bInstitute of Pathology, University Hospital Basel, 4056 Basel, Switzerland

^cDepartment of Medicine, Memorial Sloan Kettering Cancer Center, New York, NY 10065, USA

^dDepartment of Surgery, Memorial Sloan Kettering Cancer Center, New York, NY 10065, USA

^eHuman Oncology and Pathogenesis Program, Memorial Sloan Kettering Cancer Center, New York, NY 10065, USA

^fDepartment of Radiation Oncology, Memorial Sloan Kettering Cancer Center, New York, NY 10065, USA

Received 11 January 2019; revised 11 March 2019; accepted 14 March 2019

Keywords:

Salivary duct carcinoma;
ALK rearrangements;
HNRNPH3-ALK;
ERBB2 amplification;
BRCA1 germline mutation

Summary Salivary duct carcinoma (SDC) is a rare, aggressive malignancy with limited treatment options and poor outcome. Twenty-nine primary resected SDC, including 15 SDC *de novo* (SDCDN), and 14 SDC ex pleomorphic adenoma (SDCXPA) were subjected to the massive parallel sequencing assay (MSK-IMPACT) targeting 287 to 468 cancer-related genes. *TP53* was the most frequently altered gene (69%). *TP53* mutations and *ERBB2* amplification were more frequent in SDCXPA than in SDCCDN ($P = .0007$ and $P = .01$, respectively). Potentially targetable mutations were detected in 79% (23/29) of SDC involving *ERBB2* (31%), *PIK3CA* (28%), *HRAS* (21%), *ALK* (7%) and *BRAF* (3%), and 22% (5/23) of those cases harbored possible primary resistance mutations involving *CCNE1*, *NF1* and *PTEN*. A novel *HNRNPH3-ALK* rearrangement was found in one SDCCDN. In another case, *EML4-ALK* fusion detected in the primary tumor was associated with *ALK* G1202R secondary resistance mutation in the post-treatment metastasis. A germline analysis of the DNA repair genes revealed a case with a pathogenic *BRCA1* E23fs germline variant. SDCCDN and SDCXPA are genetically distinct. Although the majority of SDC may be amenable to molecular targeted therapy, concurrent possible resistance mutations may be found in a significant minority of cases. A broad genomic profiling is necessary to ensure detection of rare but clinically actionable somatic alterations in SDC.

© 2019 Elsevier Inc. All rights reserved.

[☆] Disclosure Statement: No conflict of interests exists for all contributory authors. Research reported in this publication was supported by the Cancer Center Support Grant of the National Institutes of Health/National Cancer Institute under award number P30CA008748.

* Corresponding author at: Department of Pathology, Memorial Sloan Kettering Cancer Center, 1275 York Avenue, New York, New York, 10065.
 E-mail address: dogans@mskcc.org (S. Dogan).

1. Introduction

Salivary duct carcinoma (SDC) is an aggressive malignant epithelial tumor of the salivary glands that accounts for 9% of salivary malignancies [1]. It most commonly arises in the parotid, more frequently affect men, and has a peak incidence in those older than 50 years of age. Most patients present with a rapidly progressive disease, at clinical stage III or IV. The mainstay of therapy includes surgical removal for localized disease with or without adjuvant radiotherapy and palliative chemotherapy for metastatic disease with unresectable locally recurrent tumors. The prognosis remains poor and more than 50% of patients die within 3 to 5 years of the diagnosis [2]. SDC arises either *de novo* or from a pre-existing pleomorphic adenoma (PA). Except for the presence of the residual PA component in SDCXPA, the two histologic subtypes are morphologically and immunophenotypically very similar. They both usually comprise of large apocrine tumor cells forming ducts, cribriform structures and nests with comedo-type necrosis, strikingly similar to those seen in invasive mammary carcinoma with apocrine features [3].

Several genomic studies to date have shown that the majority of SDC harbor somatic genetic alterations, namely *ERBB2* (*HER2*) amplification, and mutations in *TP53*, *PIK3CA* and *HRAS* [4,5]. In contrast to the prior studies focused on detection of possible druggable targets, studies exploring the potential mechanisms of resistance to targeted therapy in SDC are lacking. Here, we performed an in-depth genomic analysis of SDC aiming (1) to examine somatic genetic alterations in SDC relative to their putative cell of origin/precursor lesion and to predict their functional impact, and (2) to examine matched normal DNA for the presence of germline mutations in DNA repair genes. To achieve these aims, 15 SDCs *de novo* and 14 SDCs ex PA were subjected to targeted capture massively parallel sequencing (MPS) utilizing the Memorial Sloan Kettering-Integrated Mutation Profiling of Actionable Cancer Targets (MSK-IMPACT) assay [6], which interrogates somatic genetic alterations, including select rearrangements, in 287 to 468 key cancer-related genes.

2. Materials and methods

2.1. Patients and tissue samples

The study was approved by the Institutional Review Board (IRB) of Memorial Sloan Kettering Cancer Center. Signed informed consents were obtained according to the approved protocol. Twenty-nine primary resected, widely invasive SDC diagnosed between December 1999 and July 2017 with sufficient formalin-fixed paraffin-embedded (FFPE) tissue were studied including 27 conventional SDC and 2 sarcomatoid variants (SDC27 and SDC28). In 15 (52%) cases, the entire tumor was processed for microscopic examination. A diagnosis of SDCXPA was made based on the presence of histologic

evidence of pre-existing PA such as hypocellular hyalinized/sclerotic calcified nodule and/or presence of chondroid or myxoid areas with benign ductal elements [7]. In total, 15 (52%) SDCDN, including one case with tested primary and two subsequent metastases (SDC37), and 14 (48%) SDCXPA were analyzed. Four cases (SDC3, SDC30-32) were included in a prior study [5]. All cases were reviewed by two head and neck pathologists with interest and expertise in salivary gland pathology (S.D., N.K.).

2.2. DNA extraction targeted capture MPS

Genomic DNA was extracted from formalin-fixed paraffin embedded tissue curls cut at 10- μ m using the QIAamp FFPE Tissue Kit (Qiagen) 8. Fifteen (52%) SDCDN and 14 (48%) SDCXPA were subjected to targeted capture MPS using the MSK-IMPACT assay. Somatic genetic alterations in 287 (7 samples), 341 (13 samples), 410 (7 samples) or 468 (4 samples) cancer-related genes were detected using our clinically validated assay as previously described [6]. A germline analysis of DNA repair genes was performed in 11 cases (SDC27-SDC37).

2.3. Clonality, pathogenicity, and zygosity status of somatic mutations

The cancer cell fraction of each mutation was inferred using the number of reads supporting the reference and the alternate alleles and the segmented Log₂ ratio from MPS as input for ABSOLUTE (v1.0.6) [8]. Solutions from ABSOLUTE were manually reviewed as recommended [8,9]. A mutation was classified as clonal if its clonal probability, as defined by ABSOLUTE, was >50% or if the lower bound of the 95% confidence interval of its cancer cell fraction was >90% [10]. Mutations that did not meet the above criteria were considered subclonal. The pathogenicity of mutations was determined using two methods. "Method 1" was previously described [11]. (Details are provided in Supplementary Methods). The pathogenicity/oncogenic potential of other genetic alterations such as copy number alterations, gene rearrangements and intragenic deletions was determined using OncoKB annotation ("Method 2") available on cBioportal (www.cbioportal.org; Supplementary Table 2). The pathogenicity interpretation was compared between the two methods and alterations designated as likely pathogenic, potentially pathogenic, pathogenic, likely oncogenic, predicted oncogenic and oncogenic by either of the two methods were considered pathogenic/oncogenic. Actionability/targetability of genetic alterations and gene signaling pathways designation were determined using OncoKB. Allelic-specific copy number alterations and allelic-specific loss of heterozygosity (LOH) were defined using FACETS [12], which performs a joint segmentation of the total and allelic copy ratio and infers allele-specific copy number states. Regions of LOH were manually reviewed using plots of log ratios and B allele frequencies.

Table 1 Clinicopathologic features of salivary duct carcinoma

	SDCDN (N = 15)	SDCXPA (N = 14)
Men	14 (93%)	11 (79%)
Women	1 (7%)	3 (21%)
Age median (range), years	67 (51-82)	65 (31-98)
Smoking history	7 (47%)	9 (64%)
Primary site		
Parotid	15 (100%)	13 (93%)
Submandibular gland	0	1 (7%)
Tumor size mean (range), cm	3.2 (1.7-5.0)	2.5 (1.1-5.0)
AR immunoeexpression	15 (100%)	14 (100%)
Clinical stage		
I	2 (13%)	1 (7%)
II	0	1 (7%)
III	1 (7%)	2 (14%)
IV	12 (80%)	10 (71%)
Treatment		
Surgery	15 (100%)	14 (100%)
RT	15 (100%)	13 (93%)
CT	10 (67%)	7 (50%)
Anti-AR	0	2 (14%)
Anti-HER2	0	1 (7%)
ALK inhibitor	1 (7%)	0
Distant recurrence		
Bone	5 (33%)	4 (29%)
Lung	7 (47%)	2 (14%)
Brain	2 (13%)	2 (14%)
Liver	0	3 (21%)
Clinical outcome		
FU period median (range), months	31 (5-82)	13 (2-160)
Death	8 (53%)	6 (43%)
Disease-related death	6 (40%)	5 (36%)
Recurrence	9 (60%)	9 (57%)

Abbreviations: SDC, salivary duct carcinoma; SDCCN, salivary duct carcinoma *de novo*; SDCXPA, salivary duct carcinoma ex pleomorphic adenoma; AR, androgen receptor; RT, radiation therapy; CT, chemotherapy; CRT, chemotherapy and radiation therapy; FU, follow up.

2.4. Phylogenetic tree construction

A maximum parsimony tree was built for SDC37 using binary presence/absence matrices based on the repertoire of non-

synonymous and synonymous somatic mutations, gene amplifications and homozygous deletions, as described in Murugaesu et al [13] and Guerini-Rocco et al [14]. (Details are provided in Supplementary Methods).

Table 2 Genetic differences between salivary duct carcinoma *de novo* and salivary duct carcinoma ex pleomorphic adenoma

	SDC (N = 29)	SDCCN (N = 15)	SDCXPA (N = 14)	P
All somatic alterations	230	85	145	
Pathogenic/oncogenic somatic alterations	124 (54%)	63 (74%)	72 (50%)	.0003
Somatic mutations, median (range)	135, 3 (1-19)	49, 3 (1-6)	85, 4 (1-19)	
Pathogenic/oncogenic somatic mutations	91 (67%)	38 (78%)	53 (62%)	NS
CNA, median (range)	91, 1 (0-22)	32, 1 (0-15)	59, 2 (0-22)	
Oncogenic CNA	30 (33%)	11 (34%)	19 (32%)	NS
Structural variants (fusion, intragenic deletion)	5 (17%)	4 (27%)	1 (7%)	
Oncogenic structural variants	4 (80%)	3 (75%)	0	
<i>TP53</i> mutations	20 (69%)	6 (40%)	14 (100%)	.0007
Missense <i>TP53</i> mutations	9 (31%)	0	9 (64%)	.01
<i>ERBB2</i> amplification	8 (28%)	1 (7%)	7 (50%)	.01
<i>TP53</i> mutations + <i>ERBB2</i> amplification	7 (24%)	0	7 (50%)	.002

Abbreviations: SDC, salivary duct carcinoma; SDCCN, salivary duct carcinoma *de novo*; SDCXPA, salivary duct carcinoma ex pleomorphic adenoma.

2.5. Fluorescence in situ hybridization

Formalin-fixed paraffin tumor tissue 4- μ m sections were tested for *ALK* (SDC37) by fluorescence *in situ* hybridization (FISH). Tissue sections were pretreated by deparaffinizing in xylene and dehydrating in ethanol. *ALK* Break Apart FISH Probe Kit (Abbott Molecular, Des Plaines, IL) was used. Dual-color FISH was performed according to the protocol from Vysis/Abbott Molecular. FISH analysis and signal capture were performed on a fluorescence microscope (Zeiss Axioplan, Oberkochen, Germany) coupled with the ISIS FISH Imaging System (Metasystems, Waltham, MA). In *ALK* FISH study, 100 interphase nuclei from the tumor specimen were examined and a minimum of 15% cells with the rearrangement signal was required to consider a tumor positive for *ALK* rearrangement.

2.6. Immunohistochemistry

Immunohistochemistry (IHC) studies for HER2 (Ventana, clone 4B5, antibody concentration 6 μ g/ml), p40 (Biocare, mouse monoclonal antibody, dilution 1:200), *ALK* (Cell Signaling, Danvers, MA; clone D5F3, dilution 1:250) and androgen receptor (AR; Dako, monoclonal mouse antibody clone AR-441, dilution 1:100) were performed using the standard streptavidin-biotin-peroxidase procedure with the Ventana system according to the manufacturer's protocol (Ventana

Medical Systems Inc, Tucson, AZ). Appropriate positive and negative controls were used for each antibody. The immunohistochemistry results for HER2 were interpreted using the 2013 American Society of Clinical Oncologists (ASCO)/College of American Pathologists (CAP) guidelines for breast cancer [15], and cases with a score 3+ were considered HER2 positive. Androgen receptor (AR) antibody clone AR-441 (monoclonal mouse, dilution 1:100; Dako) was used to determine AR immunoreactivity. Positive nuclear labeling in at least 1% tumor cells was considered positive.

2.7. Comparison of the mutational profiles of SDC and luminal androgen receptor-positive triple-negative breast cancer

For the comparison of mutational frequencies in SDCDN and SDCXPA with 38 luminal androgen receptor-positive triple-negative breast cancer (LAR-TNBC) reported by TCGA [16], we retrieved the publicly available mutation data from cBioPortal website (<http://www.cbioportal.org/>). We restricted the comparison to only 468 genes because SDC cohorts were sequenced for only this panel of genes.

2.8. Statistical analysis

χ^2 Test or Fisher's exact test for nonparametric variables and Student *t* test for continuous variables were used for

Table 3 Spectrum of *TP53* mutations in salivary duct carcinoma

Case	Genetic alteration	Variant class	OncoKB annotation (Method 2)	OncoKB hotspot	Zygoty status	Clonal/subclonal	Pathogenicity (Method 1)
SDCDN							
SDC02	<i>TP53</i> X307_splice	Splice site	Likely onc		LOH	Clonal	Pathogenic
SDC06	<i>TP53</i> X186_splice	Splice site	Likely onc			Subclonal	Pathogenic
SDC10	<i>TP53</i> P142fs	Frameshift del	Likely onc			Subclonal	Pathogenic
SDC34	<i>TP53</i> exon 6-9 intragenic del	Intragenic del	Likely onc		LOH	NA	NA
SDC35	<i>TP53</i> F113Qfs*5	Frameshift del	Likely onc		LOH	Clonal	Likely pathogenic
SDC36	<i>TP53</i> M340Ifs*6	Frameshift ins	Likely onc		LOH	Subclonal	Likely pathogenic
SDCXPA							
SDC19	<i>TP53</i> A159V	Missense	Onc		LOH	Clonal	Pathogenic
SDC20	<i>TP53</i> R175H	Missense	Onc	Yes	LOH	Clonal	Pathogenic
SDC21	<i>TP53</i> A76fs*73	Frameshift	Likely onc			Clonal	Pathogenic
SDC22	<i>TP53</i> PH177del	Inframe del	Likely onc		LOH	Clonal	Pathogenic
SDC23	<i>TP53</i> Q167fs	Frameshift del	Likely onc		LOH	Clonal	Pathogenic
SDC24	<i>TP53</i> R175H	Missense	Onc	Yes	LOH	Clonal	Pathogenic
SDC26	<i>TP53</i> R306X	Nonsense	Likely onc			Clonal	Pathogenic
SDC27	<i>TP53</i> E346X	Nonsense	Likely onc		LOH	Clonal	Pathogenic
SDC28	<i>TP53</i> R273H	Missense	Onc	Yes	LOH	Clonal	Pathogenic
SDC29	<i>TP53</i> E258K	Missense	Likely onc		LOH	Clonal	Pathogenic
SDC30	<i>TP53</i> R175H	Missense	Onc	Yes		Subclonal	Pathogenic
SDC31	<i>TP53</i> Q331*	Missense	Likely onc		LOH	Subclonal	Likely pathogenic
SDC32	<i>TP53</i> S215G	Missense	Onc	Yes	LOH	Subclonal	Likely pathogenic
SDC33	<i>TP53</i> C238W	Missense	Likely onc	Yes	LOH	Clonal	Likely pathogenic

Abbreviations: SDC, salivary duct carcinoma; SDCDN, salivary duct carcinoma *de novo*; SDCXPA, salivary duct carcinoma ex pleomorphic adenoma; onc, oncogenic; LOH, loss of heterozygosity.

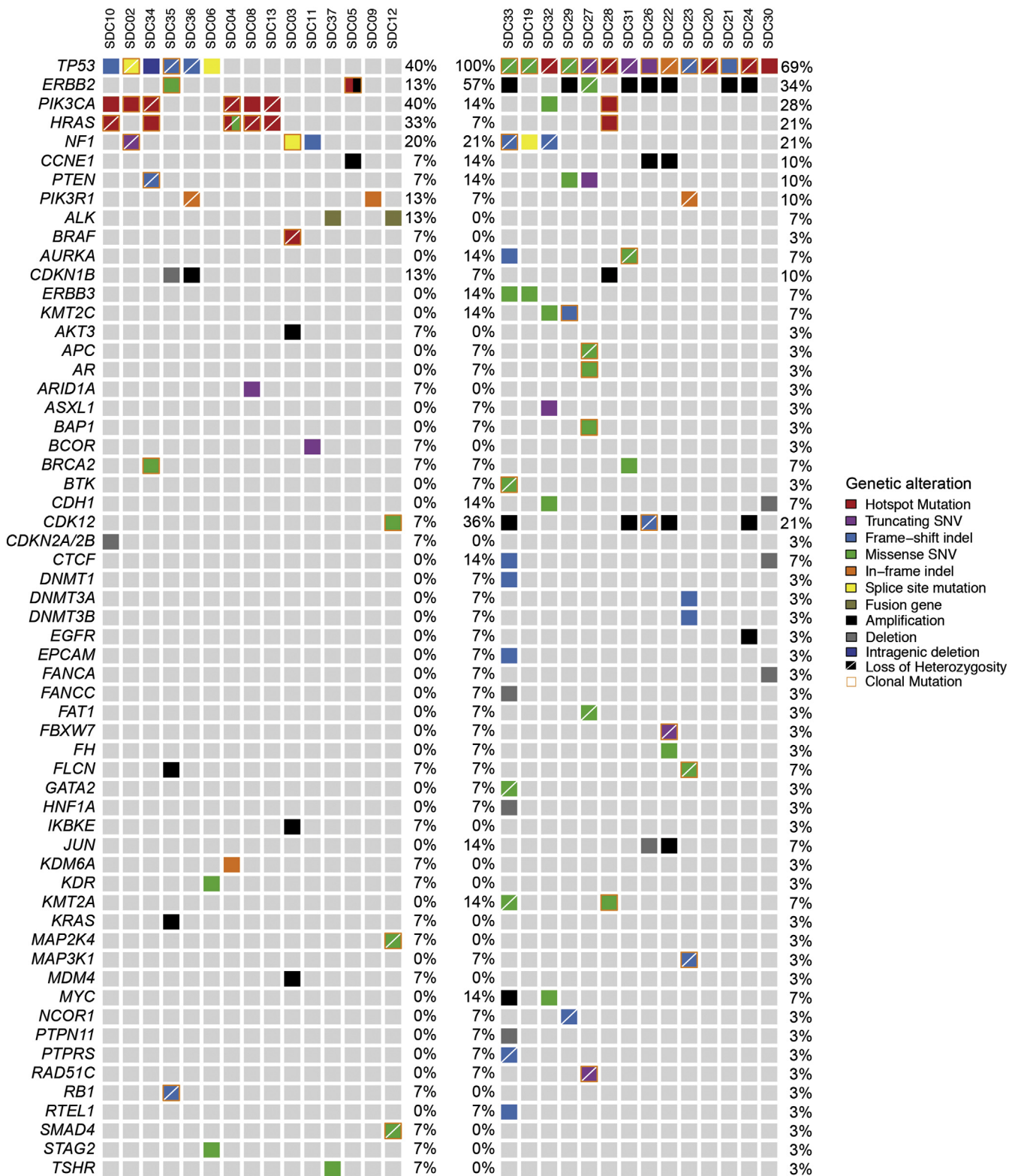


Fig. 1 The repertoire of somatic mutations in primary SDC detected by the MSK-IMPACT assay. Only genes altered by at least one pathogenic/ oncogenic mutation are listed. The top row lists all the cases. SDCDN are represented on the left panel with mutation frequencies displayed on the right, and SDCXPA are represented on the right panel with mutation frequencies displayed on the left. Mutation frequencies for the entire cohort, including both histologic subtypes, are on the far right.

statistical analyses. All tests performed were two-tailed. $P < .05$ was considered significant. Survival analysis was performed using log-rank test. Benjamini & Hochberg (BH) method was used for P value adjustment in multiple comparisons analysis.

3. Results

3.1. Clinical characteristics of SDCDN and SDCXPA

Clinicopathologic features of SDCDN and SDCXPA are summarized in Table 1. All but one patient was male, presenting at the median age of 67 years (range, 51-82) in the SDCDN group, and at 65 years (range, 31-98) in the SDCXPA group. All but one case arose in the parotid gland and all cases expressed AR. The majority of the patients in both groups presented at clinical stage IV (80% and 71%) and were treated with multimodal therapy. The median follow-up was 31 months (range, 5-82) and 13 months (range, 2-160) for carcinomas *de novo* and carcinomas ex PA, respectively. In our cohort, there were 14 deaths (48%), including 8 of 15 (53%) and 6 of 14 (43%) SDCDN and SDCXPA, respectively. Eleven patients (38%) suffered disease-related death, including 6 (50%) with SDCDN and 5 (36%) with carcinomas ex PA. A total of 17 patients (59%) had recurrence during their disease course, including 9 (60%) carcinomas *de novo* and 8 (57%) carcinomas ex PA cases. Survival analysis using log-rank test revealed no significant difference in overall survival, disease-specific survival and recurrence-free survival between *de novo* carcinomas and ex PA cases ($P = .203$, 0.117 and 0.325, respectively).

3.2. SDC displays a complex repertoire of somatic genetic alterations

A total of 31 samples from 29 SDC (including primary and two metastases in one case) were subjected to targeted capture MPS to average read depths 539-fold (range, 38-fold to 4064-fold) and 443-fold (range, 44-fold to 1967-fold) for the tumor and matched normal tissue samples, respectively. Overall, 134 somatic mutations, 91 copy number alterations, and 5 structural variants including *TP53* intragenic deletion (exons 6-9) and 3 fusion genes, *PLAG1-CTNNB1*, *EML4-ALK* and *HNRNP3-ALK* were identified among the 29 primary tumors (Supplementary Table 1). Out of 230 unique somatic genetic alterations, 124 (54%) were defined as pathogenic/oncogenic using the two methods as described above (Supplementary Fig. 1).

3.3. Genetic differences between SDCDN and SDCXPA

Genetic characteristics of SDCDN and SDCXPA are summarized in Table 2. Pathogenic/oncogenic somatic alterations

were more frequent among SDCDN than SDCXPA (74% versus 50%, $P = .0003$, Fisher's exact test, Table 2). *TP53* somatic mutations were detected in 69% (20/29) cases and were significantly more frequent in SDCXPA than in carcinomas *de novo* (14/14, 100% versus 6/15, 40%, $P = .0007$, Fisher's exact test). They were all designated as (likely) pathogenic, showed LOH in the majority (15/20, 75%) of cases, and were found to be clonal (ie, present in virtually all tumor cells) in 11 (78%) carcinomas ex PA and in 2 (33%) carcinomas *de novo*. Interestingly, missense *TP53* mutations were detected only in SDCXPA (9/14, 31% versus 0/6, $P = .01$, Fisher's exact test) and these included 6 *TP53* hotspot variants; R175H (N = 3), R273H (N = 1), S215G (N = 1) and C238W (N = 1, Table 3). *ERBB2* amplification was more common in SDCXPA (7/14, 50% versus 1/15, 7%, $P = .01$, Fisher's exact test), and tended to co-exist with *TP53* mutations only in SDCXPA but not in SDCDN (7/14, 50% versus 0/15, 0%, $P = .002$, Fisher's exact test, Table 2).

3.4. Targetable somatic mutations in SDC

The repertoire of somatic mutations in SDC is summarized in Fig. 1. Potentially targetable alterations were detected overall in 23 (79%) cases involving *ERBB2* (31%), *PIK3CA* (28%), *NF1* (21%), *HRAS* (17%), *PTEN* (10%), *ALK* (7%),

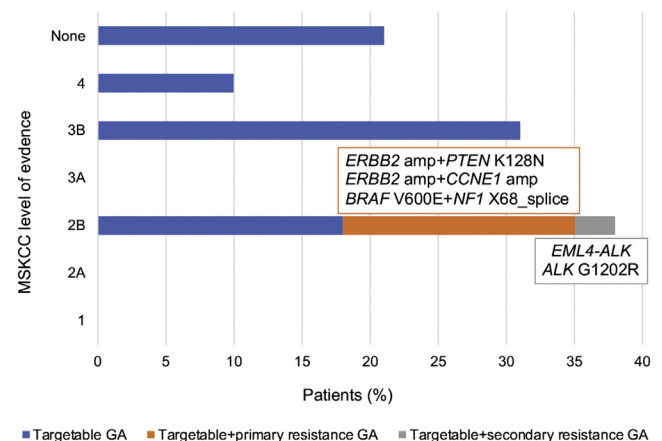


Fig. 2 Proportion of SDC patients harboring tumors with potentially targetable genetic alterations with or without possible primary or secondary resistance mutation. MSKCC levels of evidence: 1-FDA-recognized biomarker predictive of response to an FDA-approved drug in this indication, 2A-Standard care biomarker predictive of response to an FDA-approved drug in this indication, 2B-Standard care biomarker predictive of response to an FDA-approved drug in another indication, but not standard care for this indication, 3A-Compelling clinical evidence supports the biomarker as being predictive of response to a drug in this indication, but neither biomarker and drug are standard care, 3B-Compelling clinical evidence supports the biomarker as being predictive of response to a drug in another indication, but neither biomarker and drug are standard care, 4-Compelling biological evidence supports the biomarker as being predictive of response to a drug, but neither biomarker and drug are standard care. Abbreviations: amp, amplification; GA, genetic alteration.

and *BRAF* (3%); (Fig. 2, Supplementary Table 2). Oncogenic *ERBB2* alterations included *ERBB2* amplification, *ERBB2* V777 L and *ERBB2* S310F variant. The latter co-existed with *ERBB2* amplification in SDC5. Interestingly, this case displayed morphologic features of invasive lobular carcinoma of the breast but was *CDH1* wild-type (Supplementary Fig. 2). *PIK3CA* activating missense mutations affected hot-spots (E545K, E542K, H1047R, P104L, and D350G), co-existed with *HRAS* variants in 6 (21%) cases, (5 were SDCDN), and included Q61R, Q61K, G13R hotspots and one 451-2 T > G splice site variant. Coexisting *PIK3CA/HRAS* variants were found to be both clonal in 4 (67%) cases (Supplementary Table 3). *PIK3CA/HRAS* mutated tumors were morphologically similar to their *PIK3CA/HRAS*-wild-type counterparts. Twenty-six (90%) SDC cases harbored pathogenic somatic alterations in PI3K/AKT/mTOR and/or Ras/Raf/MEK/ERK signaling pathways. Among *ERBB2* copy number neutral cases, mutations in the Ras/Raf/MEK/ERK pathway were significantly more frequent than among *ERBB2* amplified cases (15/21, 71% versus 1/8, 13%, $P = .010$, Fisher's exact test, Supplementary Table 4).

3.4.1. Novel *HNRNPH3-ALK* fusion in SDCDN

A novel anaplastic lymphoma kinase (*ALK*) gene rearrangement was detected in one *de novo* carcinoma. This fusion

gene comprised of the 3' *ALK* on chromosome 2 fused to the 5' UTR of heterogeneous nuclear ribonucleoprotein H3 (2H9) (*HNRNPH3*), a gene ubiquitously expressed gene in human cells, located on chromosome 10, and resulted in a potentially functional in-frame product *HNRNPH3-ALK*. The break points mapped to exon 18 of the *ALK* gene and intron 1 of the *HNRNPH3* gene, and the chimeric protein included the entire tyrosine kinase domain of *ALK*. The disruption at the *ALK* locus was confirmed by FISH and the presence of potentially functional fusion protein was supported by positive immunohistochemistry targeting the C-terminal portion of the tyrosine kinase domain of *ALK* (Fig. 3).

3.5. Somatic mutations potentially associated with resistance to targeted therapy

Among the 23 (79%) cases harboring potential therapeutic targets, co-existing genetic alterations potentially associated with primary resistance to targeted therapies were detected in 22% (5/23) cases, ie, in 17% cases overall (5/29, Fig. 2, Supplementary Table 2). For instance, in SDC3, a *BRAF* V600E mutation was found in conjunction with a *NF1* splice site variant associated with LOH, which may cause resistance to *BRAF* V600E inhibitors [17]. Recurrent amplifications in *CCNE1*, a mechanism of resistance to anti-HER2 agents [18]

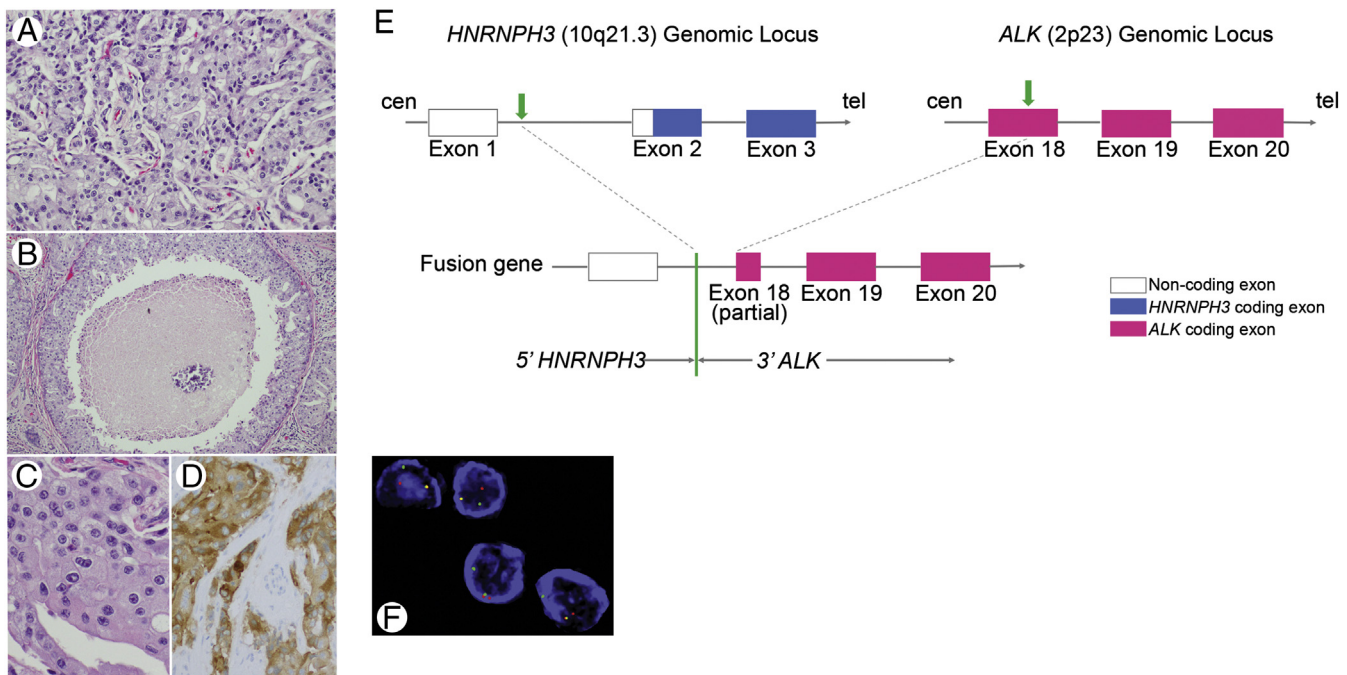


Fig. 3 SDC12 harboring *HNRNPH3-ALK* fusion formed invasive nests (H&E, medium power, A), showed comedo-type necrosis (H&E, low power, B), apocrine cytology with abundant eosinophilic cytoplasm and prominent nucleoli (H&E, high power, C), and positive cytoplasmic immunostain for ALK (high power, D). Schematic diagrams of *HNRNPH3* and *ALK* partial gene structures as well as the formation of the *HNRNPH3-ALK* fusion gene are depicted: *HNRNPH3* is located at 10q21.3 on the plus strand of chromosome 10, and *ALK* is located at 2p23 on the minus strand of chromosome 2. Transparent boxes represent noncoding parts of mature transcript of *HNRNPH3*, blue boxes represent *HNRNPH3* coding parts/exons, and red boxes represent *ALK* coding exons. Green arrows represent break points at *HNRNPH3* locus and *ALK* locus, respectively. The green line represents the fusion point of *HNRNPH3-ALK* (E). *ALK* rearrangement was confirmed by FISH (3' *ALK*, red signal, F). Abbreviations: cen, centromere; tel, telomere.

were present in 3 (14%) *ERBB2* amplified cases. *PTEN* K128 N oncogenic variant was detected in one *ERBB2* amplified case and may represent a mechanism of resistance to trastuzumab [19]. The patient with *EML4-ALK* rearranged tumor (SDC37) was treated with an investigational ALK-inhibitor and the two subsequent metastases were also genotyped. In addition to the *EML4-ALK* fusion detected in each sample, metastases harbored additional genetic alterations. A phylogenetic analysis suggested that first metastasis (m1) was substantially more genetically advanced and acquired many copy number alterations than the other lesions, while second metastasis (m2) was found with an acquired *ALK* G1202R mutation associated with secondary resistance to select ALK-inhibitors (Fig. 4).

3.6. Mutational profile of SDC is similar to that of LAR-TNBC

A comparison of mutational profiles of SDC and LAR-TNBC revealed that both tumor types are significantly enriched in mutations in *TP53* (66% versus 63%, $P = 1$, Fisher's exact test) and *PIK3CA*, (28% versus 34%, $P = .75$, Fisher's exact test, Supplementary Table 5A). However, *ERBB2* amplification was found to be significantly more frequent in SDCXPA than in LAR-TNBC (50% versus 3%, $P = .0001$, Fisher's exact test; adjusted $P = .008$, Supplementary Table 5B).

3.7. SDC patient with pathogenic germline *BRCA1* mutation

Among 11 cases (SDC27-SDC37, Supplementary Table 6) evaluated for the presence of germline DNA repair genes mutations, we identified deleterious *BRCA1* E23fs (c.68_69delAG) mutation in a 55-year-old woman with a prior history of treated high-grade papillary serous carcinoma of the ovary followed by a prophylactic bilateral mastectomy, and with maternal history of bilateral breast cancer and lung cancer (Fig. 5, Supplementary Information). Mutational profiling of the primary parotid tumor showed multiple somatic alterations including *TP53* R175H pathogenic mutation, and likely oncogenic deletions of *CDHI*, *CTCF* and *FANCA* genes, but no somatic *BRCA1* alteration (Fig. 5).

4. Discussion

Here we analyzed a series of primary resected SDCs, including SDCDN and SDCXPA, and observed that these tumors have complex genomes, with diverse patterns of gene copy number alterations, somatic mutations and fusion genes including *HNRNPH3-ALK* and *EML4-ALK* rearrangements. Despite that the majority of SDC were found with potentially targetable alterations in genes such as *ERBB2*, *PIK3CA*, *HRAS*, *ALK*, and *BRAF*, a significant minority of cases

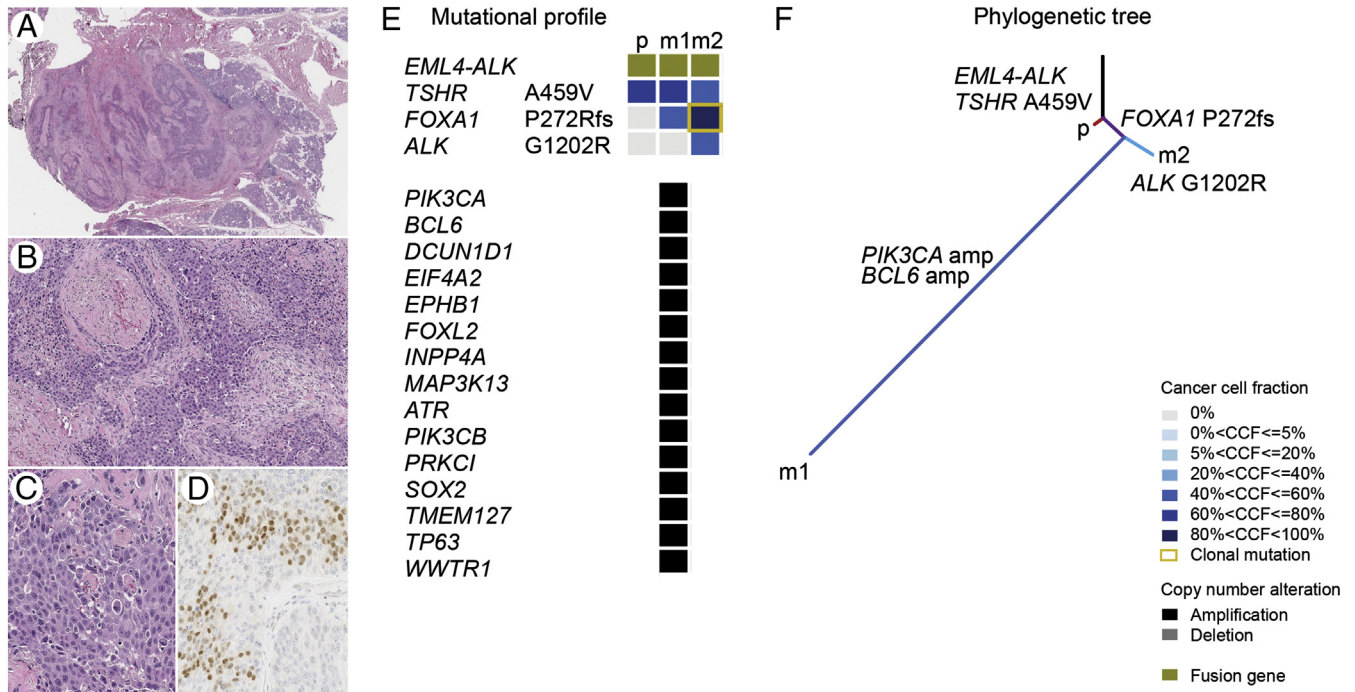


Fig. 4 SDC37 harboring *EML4-ALK* fusion gene is depicted adjacent to the normal parotid showing a diffusely infiltrative growth pattern (H&E, scanning magnification, A), perineural invasion (H&E, medium power, B), large tumor cells with abundant apocrine cytoplasm and prominent nucleoli (H&E, high power, C), and positive nuclear labeling for AR (high power, D). The distinct mutational profiles with cancer cell fractions of the primary tumor and matched metastases (E), and the phylogenetic tree illustrate the clonal evolution (F). Abbreviations: CCF, cancer cell fraction; p, primary tumor; m1, metastasis 1 (first recurrence); m2, metastasis 2 (second recurrence).

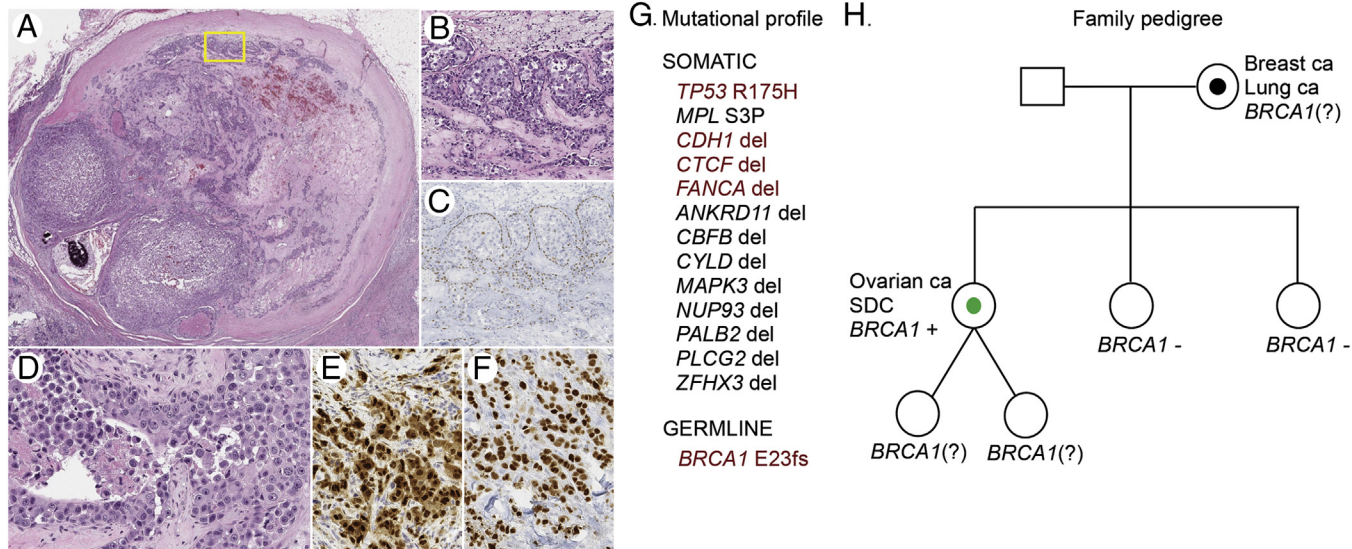


Fig. 5 Phenotype and genetics of SDC arising in a patient with a germline *BRCA1* mutation. Parotid tumor with a hyalinized nodule showing features of pre-existing PA (H&E, scanning magnification, A). The tumor cells in the in situ component at the periphery (yellow frame, A) were partly surrounded by intact benign abluminal/myoepithelial cells (H&E, medium power, B), which were positive for p63 immunostain (medium power, C). The invasive component was focally necrotic and comprised of cytologically high-grade tumor cells with prominent nucleoli and ample apocrine cytoplasm (H&E, high power, D) that were positive for AR immunostain (high power, E). Immunolabeling for p53 (F) was consistent with abnormal accumulation of mutant p53 protein due to the presence of pathogenic somatic *TP53* R175H variant (G). In addition, multiple somatic genetic alterations were detected in the sequenced tumor, while analysis of normal DNA revealed germline *BRCA1* E23fs mutation (G; pathogenic/oncogenic alterations are highlighted dark-red). The patient's family pedigree is depicted (H). Annotation: square, male; circle, female; diagonal line, twins; black dot, cancer diagnosis in a family member; green dot, cancer diagnosis, index case; (?), unknown mutation status. Abbreviations: ca, carcinoma; SDC, salivary duct carcinoma.

harbored possible primary resistance mutations involving *CCNE1*, *PTEN* and *NF1*, or a secondary resistance mutation *ALK* G1202R. Our germline analysis revealed one SDC patient harboring a pathogenic germline *BRCA1* variant.

Similar to prior studies, we identified *TP53* (69%), *ERBB2* (31%), *PIK3CA* (28%), *NF1* (21%), and *HRAS* (17%) to be the most frequently altered genes in SDC [5,20]. *ERBB2* amplification (28%) was as common as previously reported [21], identifying a significant proportion of patients potentially amenable to trastuzumab therapy [22,23]. *ERBB2* single nucleotide variants were also reported in SDC [4] and we identified two such variants, *ERBB2* V777 L and *ERBB2* S310F. *ERBB2* mutations are important to distinguish because distinct *ERBB2* variants were found to confer different sensitivity to specific anti-HER2 agents in invasive mammary carcinomas [24,25]. For example, a breast cancer patient harboring the *ERBB2* S310F in the absence of *ERBB2* amplification was reported to respond to trastuzumab [26].

While our results suggest that a significant proportion of SDC patients may be eligible for anti-HER2 targeted therapy, detection of co-existing genetic alterations as a source of primary resistance to targeted therapy may need to be considered. Out of the 8 *ERBB2* amplified cases 3 SDC showed concurrent *CCNE1* amplification and one had the *PTEN* K128 N variant; both were recognized as mechanisms of trastuzumab resistance in *ERBB2* amplified breast cancers [18,19], further implying that SDC with similar molecular profiles may not be responsive to trastuzumab therapy. A genetic similarity between SDC and invasive mammary carcinoma was suggested earlier [5,27]. Our comparison of the mutational spectra of SDC and LAR-TNBC confirmed the remarkable genetic similarity of SDC and this breast cancer subtype. Therefore, it seems reasonable to suspect that the patterns of response or resistance to targeted therapies in SDC might mirror those observed in breast cancers with a similar genetic profile.

Potential therapeutic targets were also detected in the PI3K pathway including *PIK3CA* hotspot variants in nearly one third of cases, and they frequently co-existed with *HRAS* Q61 or Q13 mutations [4,5]. SDC patients with tumors harboring mutations in PI3K pathway genes were reported to respond to PI3K/AKT/mTOR pathway inhibition [28,29]. While *PIK3CA/HRAS* mutated cases may be challenging to treat, development of dual-acting agents modulating MEK and PI3K signaling pathway has been in progress [30] suggesting that such treatment approach may eventually be explored in *PIK3CA/HRAS* mutated SDC cases.

In contrast to prior genomic studies on SDC, here we report two cases with *ALK* fusions. Fusions of the *ALK* gene with a variety of partner genes were previously found in different cancer types, including *EML4-ALK* in non-small cell lung carcinoma [31]. These fusions typically involve C-terminal tyrosine kinase domain of *ALK*, which has been a suitable target for tyrosine kinase inhibitors [32]. In the *HNRNPH3-ALK* (SDC12), the predicted transcript of this novel fusion gene includes *ALK* exons 18-29 encoding a protein comprised of the

intact kinase domain of *ALK*. Unlike most previously reported *ALK* rearrangements, which typically result from a gene to gene fusion, here the fusion point maps in the 5'UTR of *HNRNPH3*, a gene ubiquitously expressed in human cells. The expression of 3' *ALK* appears to be under the regulation of the *HNRNPH3* promoter, while the fusion transcript does not include any *HNRNPH3* coding exons. The presence of an actively translated fusion protein in the tumor cells was supported by a strong positive IHC with a monoclonal antibody targeting the C-terminal portion of the tyrosine kinase domain of *ALK*. The mechanism of *ALK* activation in *HNRNPH3-ALK* fusion resembles the one reported by Wiesner et al [33]. They described a novel *ALK* transcript containing exons 20-29 of *ALK* that were preceded by ~400 base pairs of intron 19 but not exons 1 to 19. They proposed a novel mechanism of the oncogene activation, which mapped in the intronic region and was referred to as alternative transcription initiation ("ATT") [33]. *HNRNPH3-ALK* fusion positive SDC may belong to the same group of tumors characterized by this novel mechanism of the oncogene activation.

The patient with the *EML4-ALK* rearrangement positive tumor (SDC37) was treated with an investigational *ALK*-inhibitor. He recurred with a lung metastasis harboring the *ALK* G1202R variant, which was recognized as secondary resistance mutation to select *ALK*-inhibitors in patients with *EML4-ALK* fusion positive lung adenocarcinoma [34]. While SDC patients with *ALK* rearranged tumors may benefit from *ALK* inhibition, the established knowledge on other *ALK* rearranged cancers, namely pulmonary adenocarcinomas, may help direct treatment decisions in genetically similar SDC.

In order to shed more light on the pathogenesis of SDC, we examined the differences in the mutational spectra of SDCDN and SDCXPA. To date a single study on genetic differences between SDCDN and SDCXPA using a limited gene panel has been published [20] and consistent with our results, they reported a significantly higher frequency of *TP53* mutations and *ERBB2* amplifications in SDCXPA than in *de novo* counterparts. Interestingly, we also found that certain types of *TP53* alterations were nearly restricted to one or the other histologic subtype; while missense *TP53* variants were limited only to SDCXPA, SDCDN harbored only *TP53* frame-shift truncating mutations and intragenic deletion.

In addition to the in-depth analysis of somatic alterations in SDC and in contrast to the published literature, a subset of our cohort was also examined for the presence of germline DNA repair genes mutations. We have provided the first report of a SDC patient harboring a germline *BRCA1* E23fs mutation. A single previous study has shown that the prevalence of salivary carcinoma, being salivary gland carcinoma not otherwise specified and adenoid cystic carcinoma, among *BRCA1*-mutated probands and likely carriers is significantly higher than the background incidence rate (0.052% versus 0.003%, $P < .001$) [35]. However, possible associations between germline *BRCA1/2* mutations and SDC in particular have not been previously reported.

Our study has several limitations. First, given the rarity of SDC, our cohort size is relatively small. We intentionally selected only cases with available primary tumor resection to be able to obtain the spectrum of somatic events occurring early during SDC carcinogenesis. In addition, we included only cases with available matched normal tissue (1) to obtain accurate tumor/patient-specific somatic mutational profiles, (2) to be able to perform clonality and LOH analyses of somatic variants (by FACETS), and (3) to perform a germline analysis. Second, a lack of *PLAG1/HMGA2* rearrangement status prevented us from performing additional correlations between the rearrangement status of these genes and other molecular, pathological and clinical features of SDCXPA. Third, the retrospective nature and lack of uniformity in treatment may limit the accuracy of the survival analysis. Despite the limitations several important conclusions can be drawn from the analysis made in our study. SDCDN and SDCXPA are genetically distinct. Given the complex repertoire of somatic alterations in SDC a broad genomic profiling is necessary to increase the likelihood of detection of rare but clinically actionable somatic alterations such as *ALK* fusions. Although the majority of SDC cases can be found with genetic alterations amenable to targeted therapy in “basket” clinical trials, somatic mutations associated with possible primary or secondary resistance to targeted therapies can occur in these cancers. Further studies are warranted to evaluate the risk of SDC in *BRCA1* carriers.

Supplementary data

Supplementary data to this article can be found online at <https://doi.org/10.1016/j.humpath.2019.03.004>.

Acknowledgements

We wish to acknowledge the expert help of Zoran Perak and thank him for his assistance in figures preparation.

References

- [1] Kleinsasser O, Klein HJ, Hubner G. Salivary duct carcinoma. A group of salivary gland tumors analogous to mammary duct carcinoma. *Arch Klin Exp Ohren Nasen Kehlkopfheilkd* 1968;192:100-5.
- [2] Boon E, Bel M, van Boxtel W, et al. A clinicopathological study and prognostic factor analysis of 177 salivary duct carcinoma patients from the Netherlands. *Int J Cancer* 2018;143:758-66.
- [3] Katabi N, Gomez D, Klimstra DS, et al. Prognostic factors of recurrence in salivary carcinoma ex pleomorphic adenoma, with emphasis on the carcinoma histologic subtype: a clinicopathologic study of 43 cases. *HUM PATHOL* 2010;41:927-34.
- [4] Chiosea SI, Williams L, Griffith CC, et al. Molecular characterization of apocrine salivary duct carcinoma. *Am J Surg Pathol* 2015;39:744-52.
- [5] Dalin MG, Desrichard A, Katabi N, et al. Comprehensive molecular characterization of salivary duct carcinoma reveals actionable targets and similarity to apocrine breast Cancer. *Clin Cancer Res* 2016;22:4623-33.
- [6] Cheng DT, Mitchell TN, Zehir A, et al. Memorial Sloan Kettering-integrated mutation profiling of actionable Cancer targets (MSK-IMPACT): a hybridization capture-based next-generation sequencing clinical assay for solid tumor molecular oncology. *J Mol Diagn* 2015;17:251-64.
- [7] El-Naggar AK, Chan JKC, Grandis JR, et al. World Health Organization classification of head and neck Tumours. 4th ed. Lyon: International Agency for Research on Cancer (IARC); 2017. p. 173-5.
- [8] Carter SL, Cibulskis K, Helman E, et al. Absolute quantification of somatic DNA alterations in human cancer. *Nat Biotechnol* 2012;30:413-21.
- [9] Landau DA, Carter SL, Stojanov P, et al. Evolution and impact of subclonal mutations in chronic lymphocytic leukemia. *Cell* 2013;152:714-26.
- [10] Piscuoglio S, Ng CK, Murray MP, et al. The genomic landscape of male breast cancers. *Clin Cancer Res* 2016;22:4045-56.
- [11] Ng CKY, Piscuoglio S, Geyer FC, et al. The landscape of somatic genetic alterations in metaplastic breast carcinomas. *Clin Cancer Res* 2017;23:3859-70.
- [12] Shen R, Seshan VE. FACETS: allele-specific copy number and clonal heterogeneity analysis tool for high-throughput DNA sequencing. *Nucleic Acids Res* 2016;44:e131.
- [13] Murugaesu N, Wilson GA, Birkbak NJ, et al. Tracking the genomic evolution of esophageal adenocarcinoma through neoadjuvant chemotherapy. *Cancer Discov* 2015;5:821-31.
- [14] Guerini-Rocco E, Piscuoglio S, Ng CK, et al. Microglandular adenosis associated with triple-negative breast cancer is a neoplastic lesion of triple-negative phenotype harbouring TP53 somatic mutations. *J Pathol* 2016;238:677-88.
- [15] Wolff AC, Hammond MEH, Hicks DG, et al. Recommendations for human epidermal growth factor receptor 2 testing in breast cancer: American Society of Clinical Oncology/College of American Pathologists clinical practice guideline update. *Arch Pathol Lab Med* 2013;138:241-56.
- [16] Cancer Genome Atlas Network. Comprehensive molecular portraits of human breast tumours. *Nature* 2012;490:61.
- [17] Whittaker SR, Theurillat JP, Van Allen E, et al. A genome-scale RNA interference screen implicates NF1 loss in resistance to RAF inhibition. *Cancer Discov* 2013;3:350-62.
- [18] Scaltriti M, Eichhorn PJ, Cortés J, et al. Cyclin E amplification/overexpression is a mechanism of trastuzumab resistance in HER2+ breast cancer patients. *Proc Natl Acad Sci* 2011;108:3761-6.
- [19] de Melo Gagliato D, Jardim DL, Marchesi MS, et al. Mechanisms of resistance and sensitivity to anti-HER2 therapies in HER2+ breast cancer. *Oncotarget* 2016;7:64431-46.
- [20] Chiosea SI, Thompson LD, Weinreb I, et al. Subsets of salivary duct carcinoma defined by morphologic evidence of pleomorphic adenoma, *PLAG1* or *HMGA2* rearrangements, and common genetic alterations. *Cancer* 2016;122:3136-44.
- [21] Glisson B, Colevas AD, Haddad R, et al. HER2 expression in salivary gland carcinomas: dependence on histological subtype. *Clin Cancer Res* 2004;10:944-6.
- [22] Limaye SA, Posner MR, Krane JF, et al. Trastuzumab for the treatment of salivary duct carcinoma. *Oncologist* 2013;18:294-300.
- [23] Nabili V, Tan JW, Bhuta S, et al. Salivary duct carcinoma: a clinical and histologic review with implications for trastuzumab therapy. *Head Neck* 2007;29:907-12.
- [24] Bose R, Kavuri SM, Searleman AC, et al. Activating HER2 mutations in HER2 gene amplification negative breast cancer. *Cancer Discov* 2013;3:224-37.
- [25] Ben-Baruch NE, Bose R, Kavuri SM, et al. HER2-mutated breast cancer responds to treatment with single-agent Neratinib, a second-generation HER2/EGFR tyrosine kinase inhibitor. *J Natl Compr Canc Netw* 2015;13:1061-4.
- [26] Chumsri S, Weidler J, Ali S, et al. Prolonged response to trastuzumab in a patient with HER2-nonamplified breast cancer with elevated HER2

- dimerization harboring an ERBB2 S310F mutation. *J Natl Compr Canc Netw* 2015;13:1066-70.
- [27] Di Palma S, Simpson RH, Marchiò C, et al. Salivary duct carcinomas can be classified into luminal androgen receptor-positive, HER2 and basal-like phenotypes. *Histopathology* 2012;61:629-43.
- [28] Nardi V, Sadow PM, Juric D, et al. Detection of novel actionable genetic changes in salivary duct carcinoma helps direct patient treatment. *Clin Cancer Res* 2013;19:480-90.
- [29] Piha-Paul SA, Cohen PR, Kurzrock R. Salivary duct carcinoma: targeting the phosphatidylinositol 3-kinase pathway by blocking mammalian target of rapamycin with temsirolimus. *J Clin Oncol* 2011;29:e727-30.
- [30] Van Dort ME, Hong H, Wang H, et al. Discovery of bifunctional oncogenic target inhibitors against allosteric mitogen-activated protein kinase (MEK1) and phosphatidylinositol 3-kinase (PI3K). *J Med Chem* 2016;59:2512-22.
- [31] Soda M, Choi YL, Enomoto M, et al. Identification of the transforming EML4-ALK fusion gene in non-small-cell lung cancer. *Nature* 2007;448:561-6.
- [32] Shaw AT, Yeap BY, Solomon BJ, et al. Effect of crizotinib on overall survival in patients with advanced non-small-cell lung cancer harbouring ALK gene rearrangement: a retrospective analysis. *Lancet Oncol* 2011;12:1004-12.
- [33] Wiesner T, Lee W, Obenauf AC, et al. Alternative transcription initiation leads to expression of a novel ALK isoform in cancer. *Nature* 2015;526:453-7.
- [34] Katayama R, Shaw AT, Khan TM, et al. Mechanisms of acquired crizotinib resistance in ALK-rearranged lung cancers. *Sci Transl Med* 2012;4:120ra117.
- [35] Shen TK, Teknos TN, Toland AE, et al. Salivary gland cancer in BRCA-positive families: a retrospective review. *JAMA Otolaryngol Head Neck Surg* 2014;140:1213-7.